Efficient Dual-Phase Visual Detection of Pesticides in Real Samples with Electron-rich Emitters Carrying Multiple Twists

*Shivani Tripathi and Manab Chakravarty**

Department of Chemistry, Birla Institute of Technology and Sciences-Pilani, Hyderabad Campus, Jawaharnagar, Medak, Shamirpet, Hyderabad-500078.

Contents

Materials and Methods

General Experimental Information

All the required chemicals were purchased from various companies and used without purification. All the products were characterized by ^{1}H, and ^{13}C NMR spectroscopy. NMR spectra were recorded on a Bruker 400 MHz instrument (400 MHz for ^{1}H NMR, and 101 MHz for ^{13}C NMR). ^{1}H NMR experiments are reported in units, parts per million (ppm), and were measured relative to residual DMSO (2.50 ppm) in the deuterated solvent. ^{13}C NMR spectra are reported in ppm relative to deuteron DMSO (39.52 ppm) and all were obtained with ^{1}H decoupling. Coupling constants were reported in Hz. Reactions were monitored by thin-layer chromatography (TLC). liquid chromatography-mass spectrometry (LC-MS) was obtained by the electron spray ionization (ESI) technique using the Q-TOF mass analyzer and was reported as m/z (relative intensity). Melting points of compounds were recorded on a KRUSS Optronic M3000 apparatus.

Synthesis of (*E*)-4-(2-(10-(4-(diphenylamino) phenyl) anthracen-9-yl) vinyl)-N, N-diphenylaniline (**TT1**)., 4-((*E*)-2-(10-(4-(diphenylamino) phenyl) anthracen-9-yl) vinyl)-N-(4-((*E*)-2-(10-(4-(diphenylamino) phenyl) anthracen-9-yl) vinyl) phenyl)-N-phenylaniline (**TT2**), and 4-(10-((*E*)-4-(bis(4-((*E*)-2-(10-(4-(diphenylamino) phenyl) anthracen-9-yl) vinyl) phenyl) amino) styryl) anthracen-9-yl)-N, N-diphenylaniline (**TT3**).

The molecules **TT1, TT2** and **TT3** were synthesised via the reported protocol [1]

Thermogravimetric studies

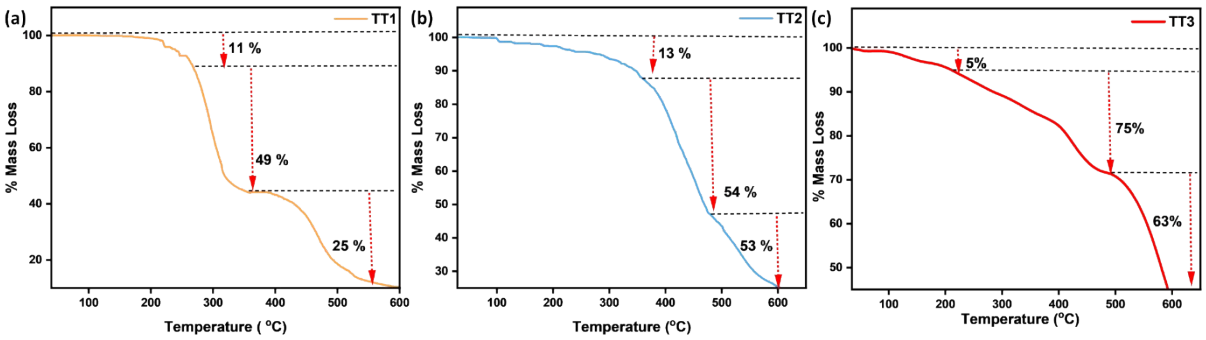

Figure S1. Thermogravimetric analysis of **(a) TT1, (b) TT2 and (c) TT3.**

PXRD Analysis

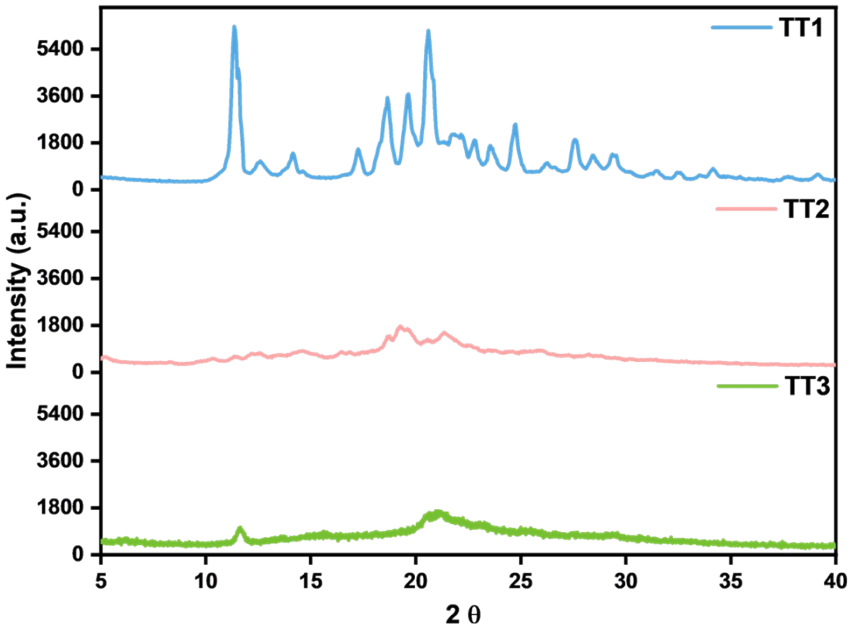

Figure S2. Comparative PXRD patterns of **TT1**, **TT2** and **TT3.**

Photophysical Studies

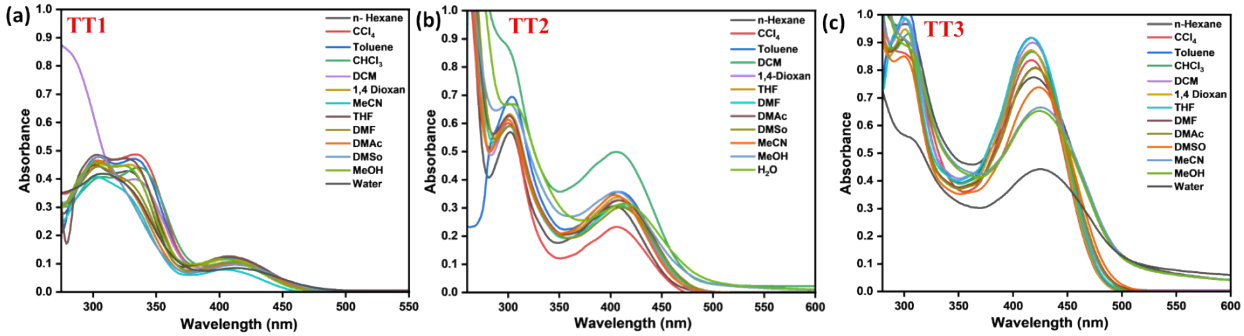

Figure S3. UV-Vis spectrum of **TT1, TT2** and **TT3** in different solvents.

Table S1. Tabulated photophysical parameters of **TT1, TT2** and **TT3** in different solvents.

Entry	Solvents	TT1		TT2		TT3	
		λ_{emi} (nm)	Φ_f (%)*	λ_{emi} (nm)	Φ_f (%)*	λ_{emi} (nm)	Φ_f (%)*
a	N-Hexane	383	28	516	11	527	16
b	Carbontetrachloride	443	4	525	6	529	12
c	Toluene	414	51	531	23	532	28
d	Dichloromethane	459	53	548	6	556	8
e	Chloroform	451	51	540	7	543	11
f	1,4-dioxan	423	61	530	14	533	20
g	Tetrahydrofuran	427	51	537	22	543	26
h	N,N-Dimethylacetamide	445	44	558	16	574	22
i	N,N-Dimethylsulphoxide	458	3	564	3	585	5
j	Dimethylformamide	452	37	558	3	545	5
k	Acetonitrile	425	5	539	1	527	4
l	Methanol	524	1	534	2	510	3
m	Water	557	1	558	1	549	2

The relative quantum yield of the probe was measured with respect to quinine sulfate (in 0.1 M H_2SO_4) using the formula,

$$\Phi_f = \Phi_f \times \frac{a_{ref}}{a_{sam}} \times \frac{A_{sam}}{A_{ref}} \times \left(\frac{n_{sam}}{n_{ref}}\right)^2$$

Where, Φ_f = quantum yield of probe Φ_{ref} = quantum yield of quinine sulfate (0.54)

A_{ref} = area under curve of emission spectra of quinine sulfate in 0.1M H_2SO_4, A*sam* = area under curve of emission spectra of probe, a_{sam} = Absorbance of probe, a_{ref} = Absorbance of quinine sulfate in 0.1M H_2SO_4, n_{sam} = refractive index of respective solvents, n_{sam} = refractive index of water.

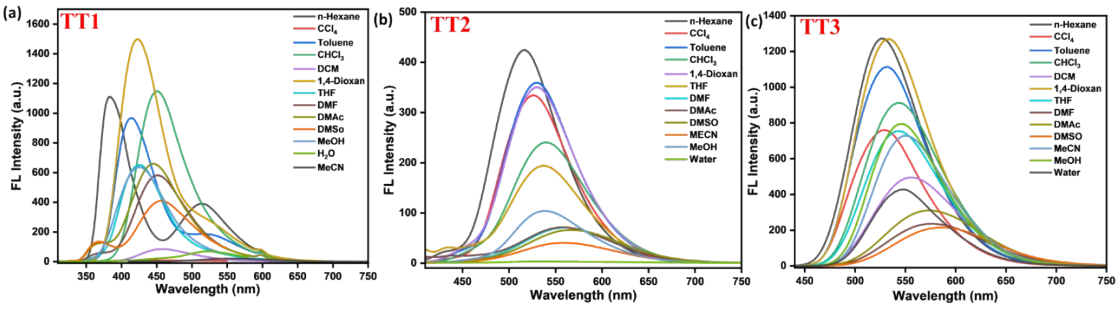

Figure S4. Emission spectra of (a) **TT1,** (b) **TT2,** and (c) **TT3** in different solvents.

Selectivity experiment for TT2 and TT3.

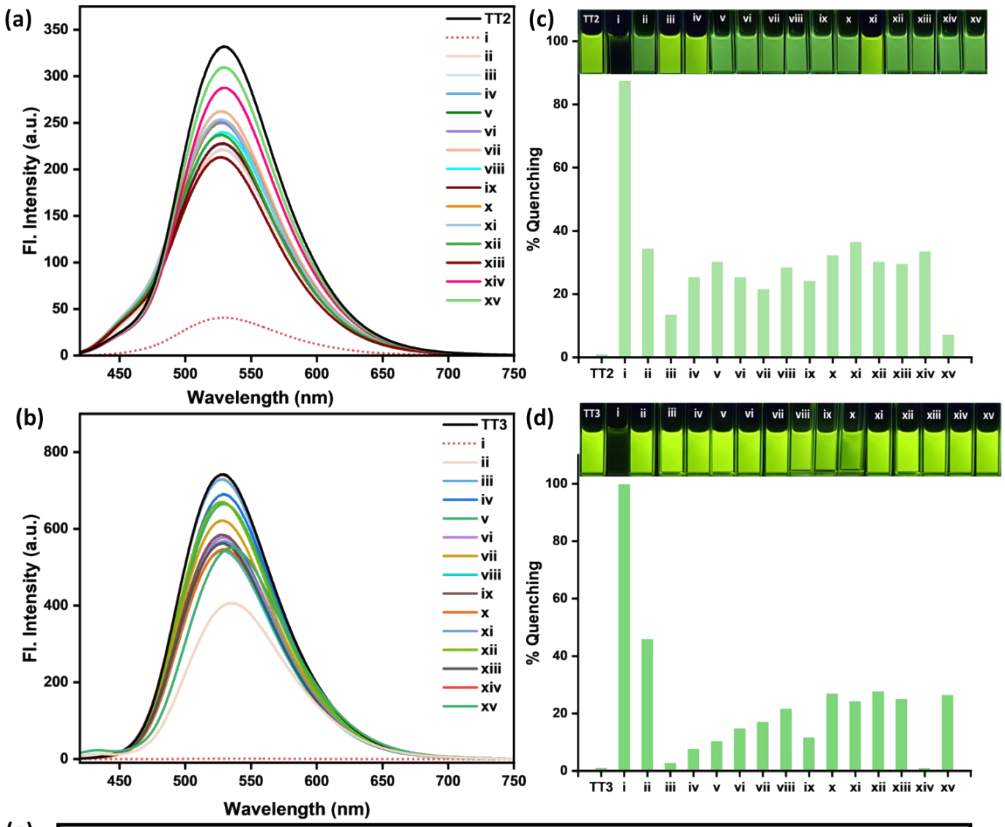
(a)
Fl. Intensity (a.u.)
Wavelength (nm)
TT2
i
ii
iii
iv
v
vi
vii
viii
ix
x
xi
xii
xiii
xiv
xv
(b)
Fl. Intensity (a.u.)
Wavelength (nm)
TT3
(c)
% Quenching
(d)
% Quenching

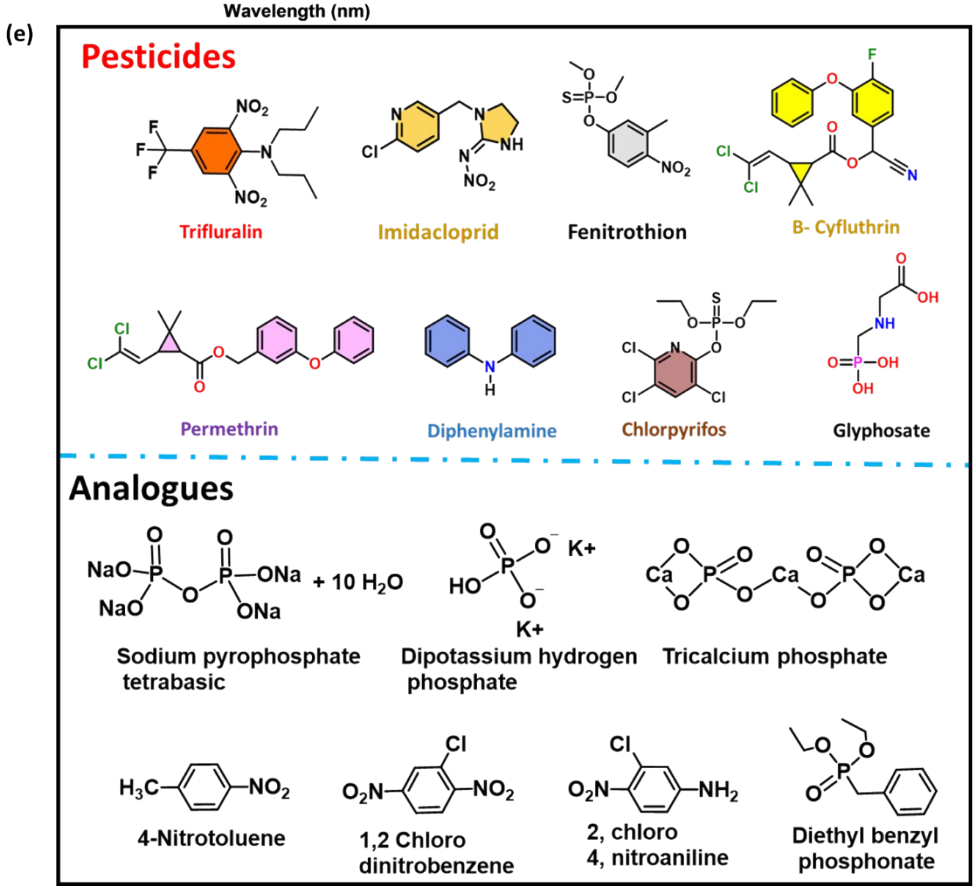
(e)
Pesticides
Trifluralin
Imidacloprid
Fenitrothion
B- Cyfluthrin
Permethrin
Diphenylamine
Chlorpyrifos
Glyphosate
Analogues
Sodium pyrophosphate tetrabasic
Dipotassium hydrogen phosphate
Tricalcium phosphate
4-Nitrotoluene
1,2 Chloro dinitrobenzene
2, chloro 4, nitroaniline
Diethyl benzyl phosphonate

Figure S5. Fl. Emission spectra of (a) **TT2**, (b) **TT3** after adding all the analytes; bar diagram representing the % quenching of (c) **TT2** (d) **TT3** (inset is photograph of **TT2** and **TT3** (10 μM in 1,4-dioxane) after treatment with various analytes): i. Trifluralin, ii. Fenitrothion, iii. Imidacloprid, iv. β-cyfluthrin, v. Chlorpyrifos, vi. Glyphosate, vii. Permethrin, viii. Diphenylamine, ix. Sodium pyrophosphate tetrabasic, x. Dipotassium hydrogen phosphate, xi. Tricalcium phosphate, xii l. 4-Nitrotoluene, xiii. 1,2-Chloro dinitrobenzene, xiv. 2-Chloro-4-nitroaniline, xv. Diethylbenzyl phosphonate. (e) molecular structure of various pesticides and other analogues used for selectivity.

Titration studies

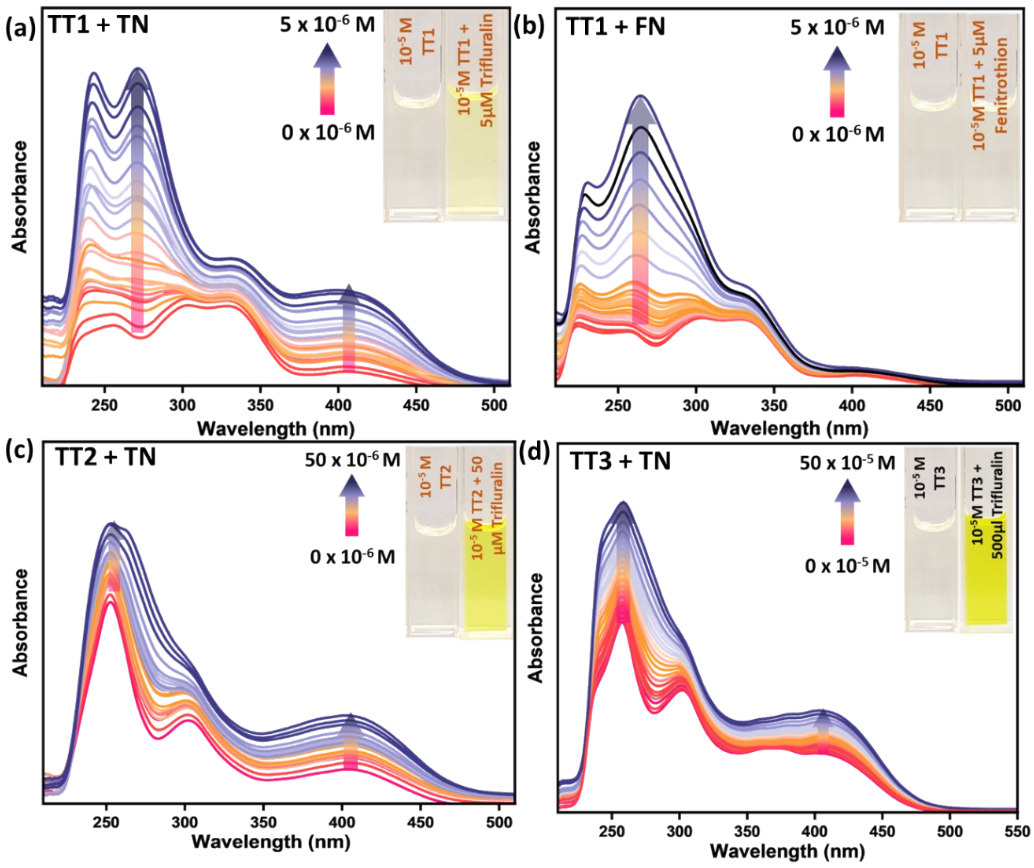

Figure S6. Change in UV-Vis spectra of **TT1, TT2** and **TT3** by gradual addition of TN and FN, respectively; Inset pictures correspond to before and after pesticide addition in ambient light.

NMR Studies

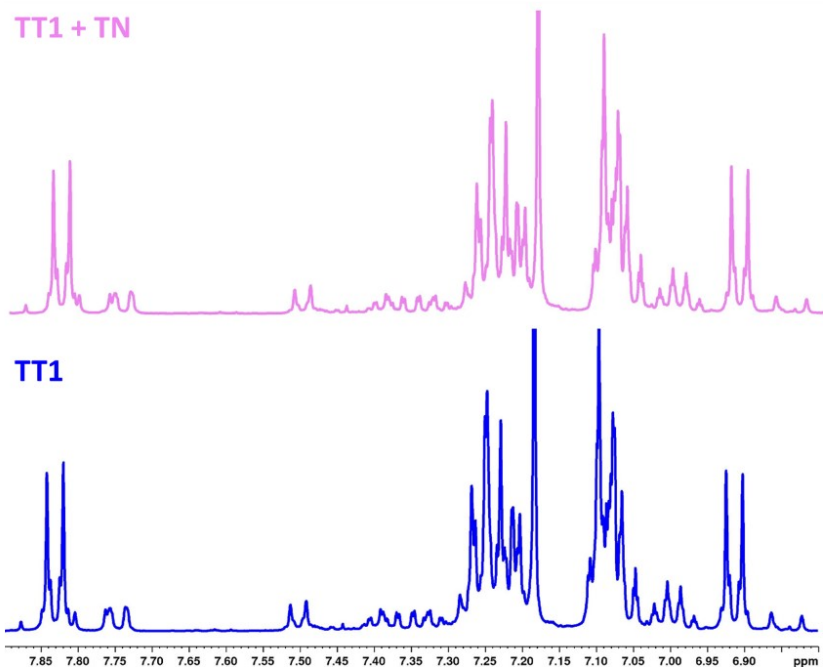

Figure S7. ^{1}H NMR (partial) spectra of **TT1** in $CDCl_3$ before (TT1) and after (TT1+TN) the addition of TN (1 equiv.).

Stern Volmer plot for TT1 TT2 and TT3

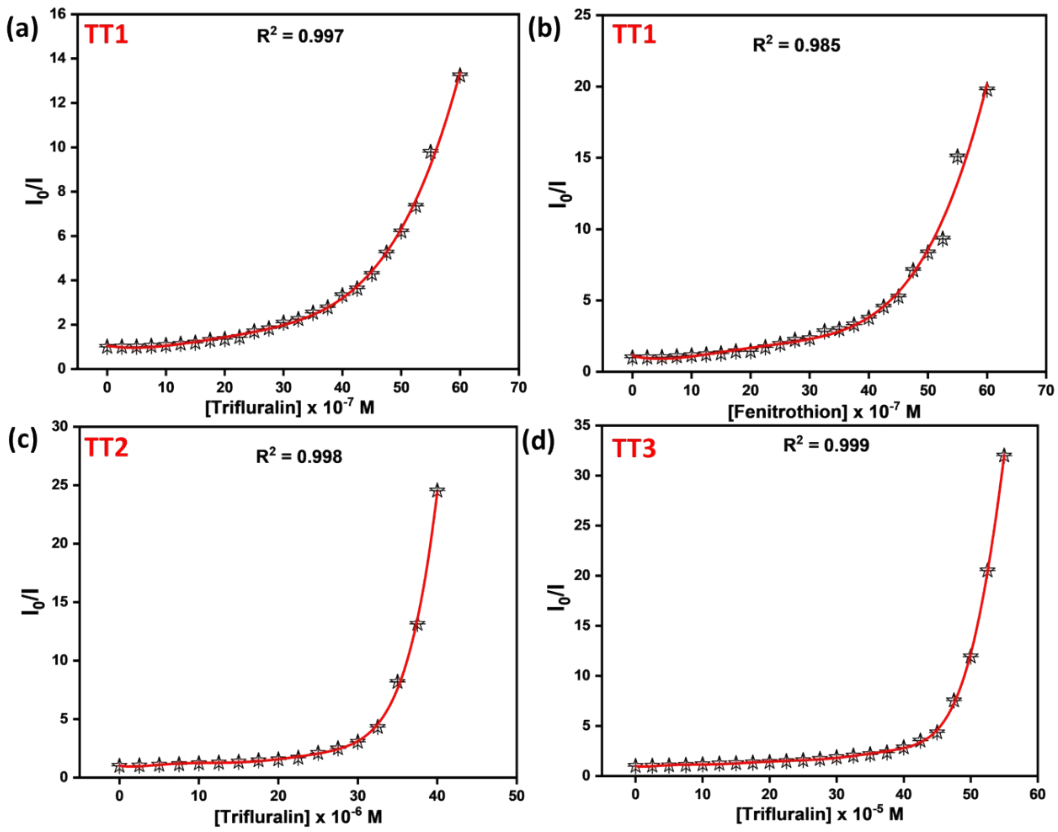

Figure S8. Stern-Volmer plots for different pesticides with (a) **TT1+TN**, (b) **TT1+FN**, (c) **TT2+TN,** (d) **TT3+TN**, in 1,4-dioxane plotting I_o/I against concentration of pesticide.

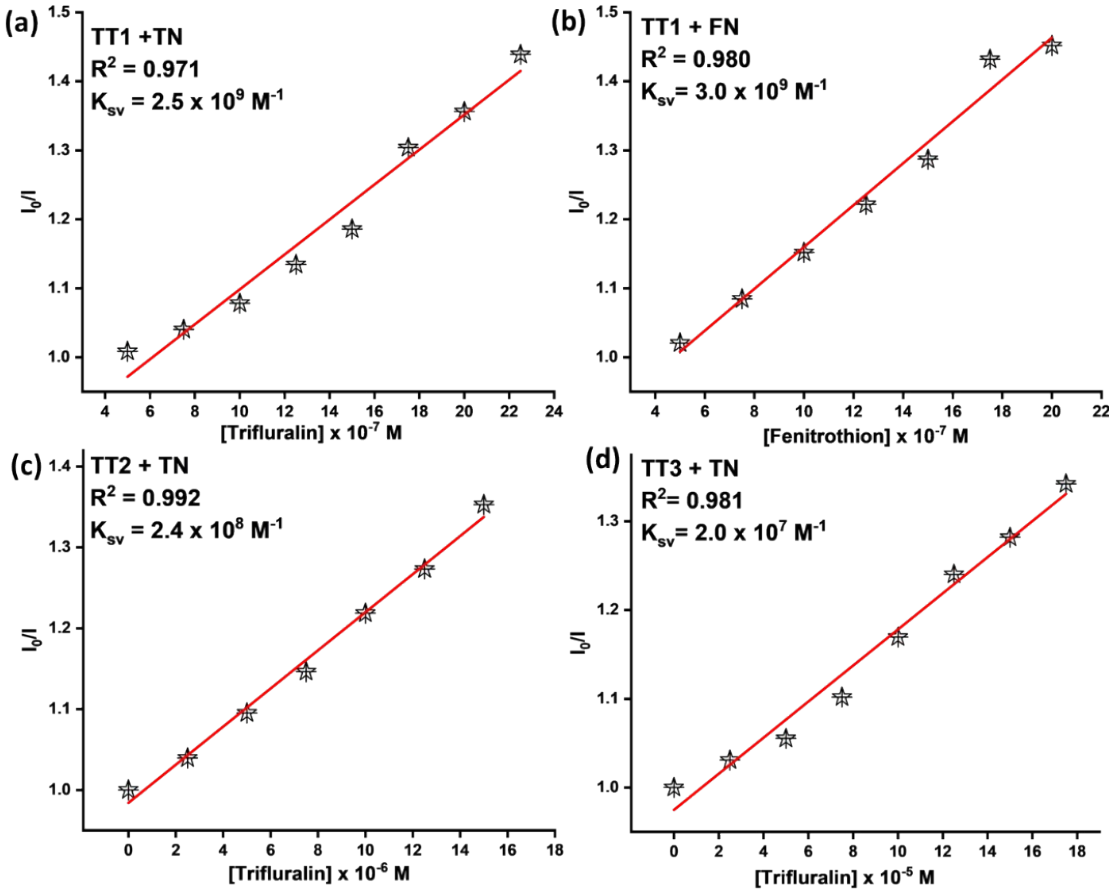

Figure S9. Stern-Volmer plots for different pesticides at lower concentration for K_{sv} (Stern-Volmer constant) determination with (a) **TT1+TN,** (b) **TT1+FN,** (c) **TT2+TN,** (d)**TT3+TN**, in 1,4-dioxane plotting I_o/I against concentration of pesticide.

Lifetime studies

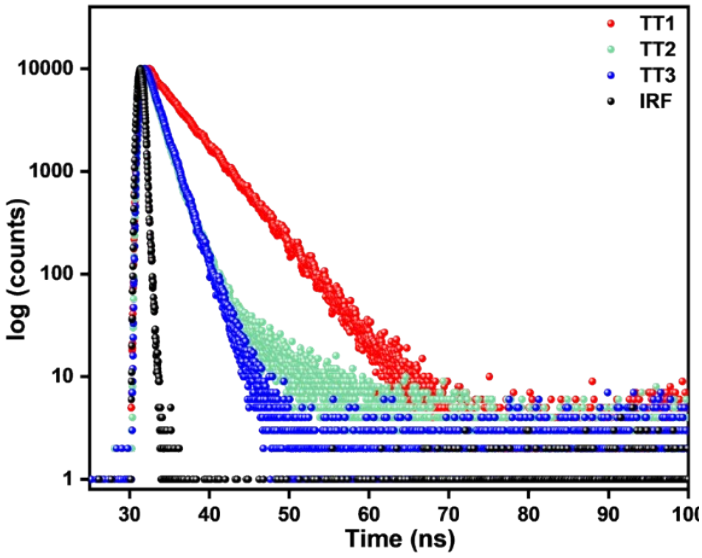

Figure S10. Lifetime decay profile of **TT1, TT2** and **TT3** (10 µM in 1,4-dioxane) in solution state.

Table S2. Lifetime decay parameters for **TT1, TT2** and **TT3** (10 µM in 1,4-dioxane) in solution state.

Sample	τ_1	τ_2	α_1	α_2	Avg.$<\tau>$ (ns)	χ^2	$\boldsymbol{\Phi_f}$ **(%)**	k_r $(10^6\ s^{-1})$	k_{nr} $(10^6\ s^{-1})$
10 µM **TT1**	2.40	4.55	0.03	0.97	4.52	1.3	**61**	134.9	86.2
10 µM **TT2**	1.63	6.59	0.99	0.01	1.88	0.9	**14**	74.4	457.4
10 µM **TT3**	1.55	2.09	0.65	0.35	1.78	0.9	**20**	112.3	449.4

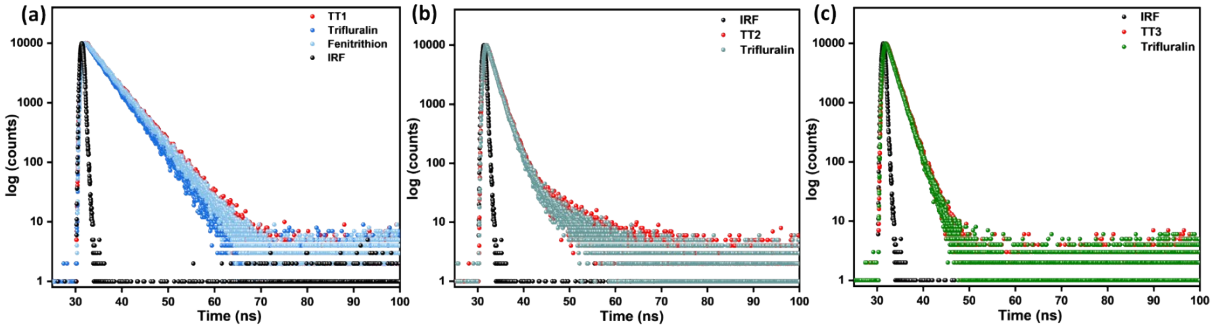

Figure S11. Lifetime decay profile of (a)**TT1**, (b)**TT2** and (c)**TT3** before and after the addition of pesticides.

Table S3. Lifetime decay parameters for **TT1, TT2** and **TT3** (10 μM in 1,4-dioxane) before and after the addition of pesticides (TN and FN).

Sample	τ_1	τ_2	α_1	α_2	Avg.<τ> (ns)	χ^2
10 μM **TT1**	2.40	4.55	0.03	0.97	**4.52**	1.3
10 μM **TT1**+5 x 10^{-6} M TN	1.74	4.31	0.07	0.93	**4.23**	1.1
10 μM **TT1**+5 x 10^{-6} M FN	3.25	4.48	0.04	0.96	**4.43**	1.2
10 μM **TT2**	1.63	6.59	0.99	0.01	**1.88**	0.9
10 μM **TT2**+50 x 10^{-6} M TN	2.13	1.25	0.39	0.61	**1.71**	1.5
10 μM **TT3**	1.55	2.09	0.65	0.35	**1.78**	0.9
10 μM **TT2**+5 x 10^{-5} M TN	1.92	1.43	0.55	0.45	**1.73**	0.9

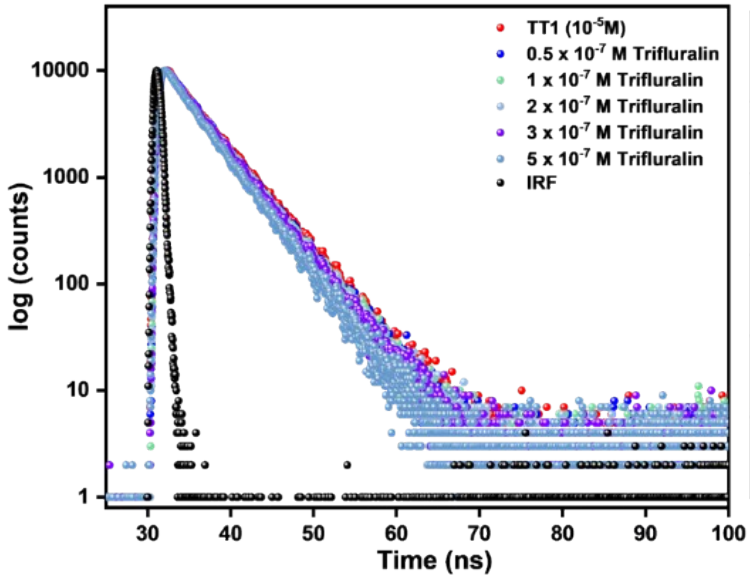

Figure S12. Lifetime decay profile of **TT1**, upon gradual addition of Trifluralin.

Table S4. Lifetime decay parameters for **TT1, TT2** and **TT3** (10 μM in 1,4-dioxane) upon gradual addition of TN.

Sample	τ_1	τ_2	α_1	α_2	Avg.<τ> (ns)	χ^2
10 μM **TT1**	2.40	4.55	0.03	0.97	**4.52**	1.3
10 μM **TT1**+ 0.5 x 10^{-7} M TN	2.23	4.44	0.06	0.94	**4.37**	1.0

10 µM **TT1**+ 1 x 10^{-7} M TN	1.71	4.39	0.05	0.95	**4.35**	0.9
10 µM **TT1**+ 2 x 10^{-6} M TN	1.83	4.32	0.05	0.95	**4.27**	1.0
10 µM **TT1**+5 x 10^{-6} M TN	1.74	4.31	0.07	0.93	**4.23**	1.1

Limit of Detection Plots for TT1, TT2 and TT3

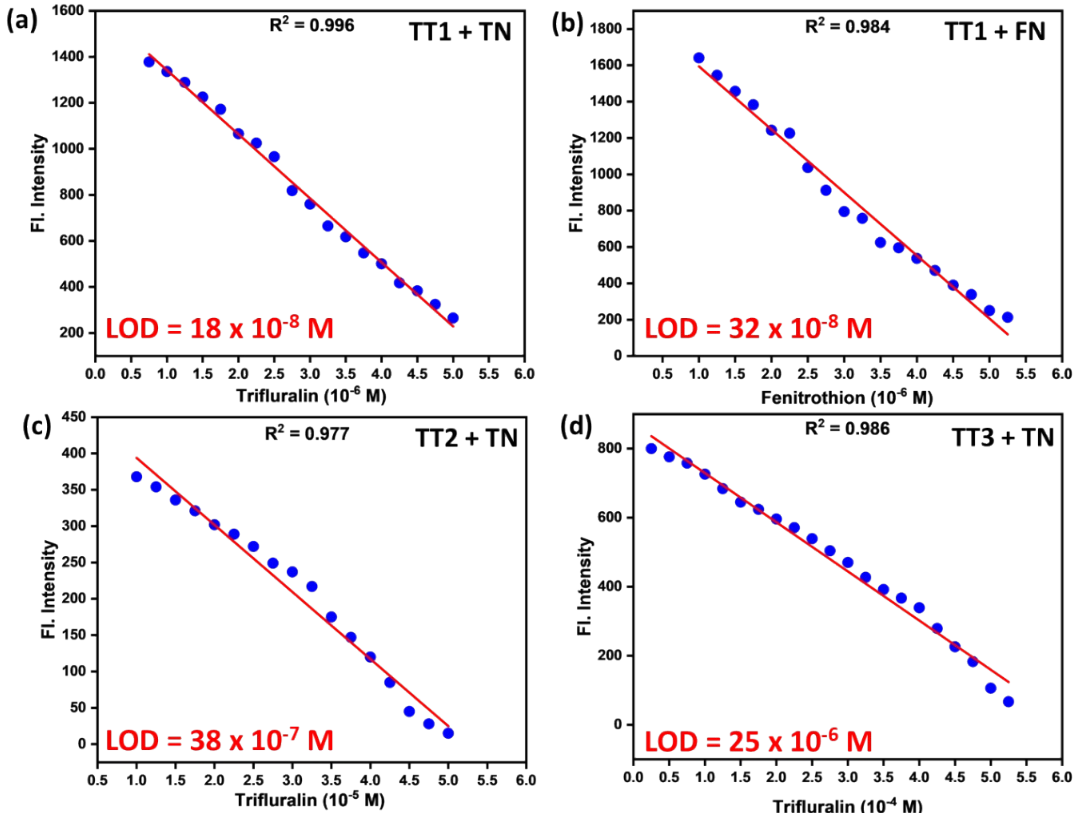

Figure S13. Limit of detection plot of different pesticides with **TT1, TT2** and **TT3** (10 µM in 1,4-dioxane)

Calculation of the Limit of Detection (LOD):

The standard deviation and slope were obtained by plotting the ratio of Fl intensity at 423, 530, 533 nm for **TT1, TT2, TT3** respectively with a concentration of pesticides

LOD = 3.3 σ/K

Where, σ = Standard error of the linear fitting and K = Slope

Example: For Trifluralin, σ = 17.46 and K = 278 x 10^6 M^{-1}, thus LOD= $\frac{3\ x\ 17.46}{278\ x\ 10^6}$ = 18 x 10^{-8} M

JOBS plot for binding ratio

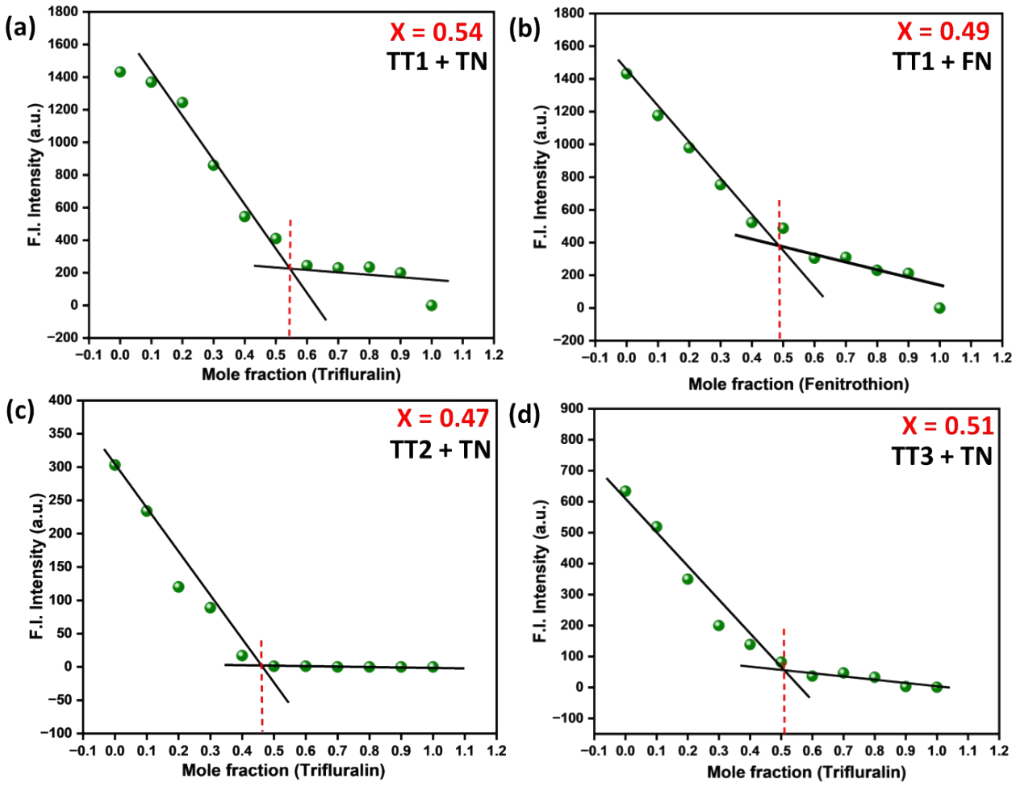

Figure S14. Fluorescence Job's plot of (a) **TT1+TN, (b)TT1+FN, (c)TT2+TN** and (d)**TT3+TN** with different pesticides, depicting 1:1 complex.

Comparative $E_{HOMO} - E_{LUMO}$ energy of TT1, TT2 and TT3.

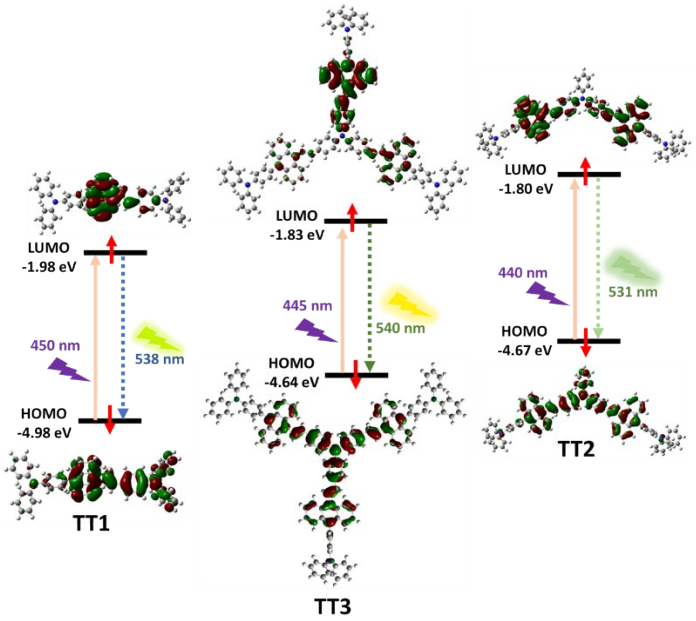

Figure S15. HOMO-LUMO energy diagrams and their respective values of **TT1, TT2,** and **TT3**. Note: The E_{HOMO}-E_{LUMO} of **TT1** was calculated theoretically as explained below. All the

calculations were performed in Gaussian using B3LYP-D3(BJ)/6-31G** (with dispersion corrections).

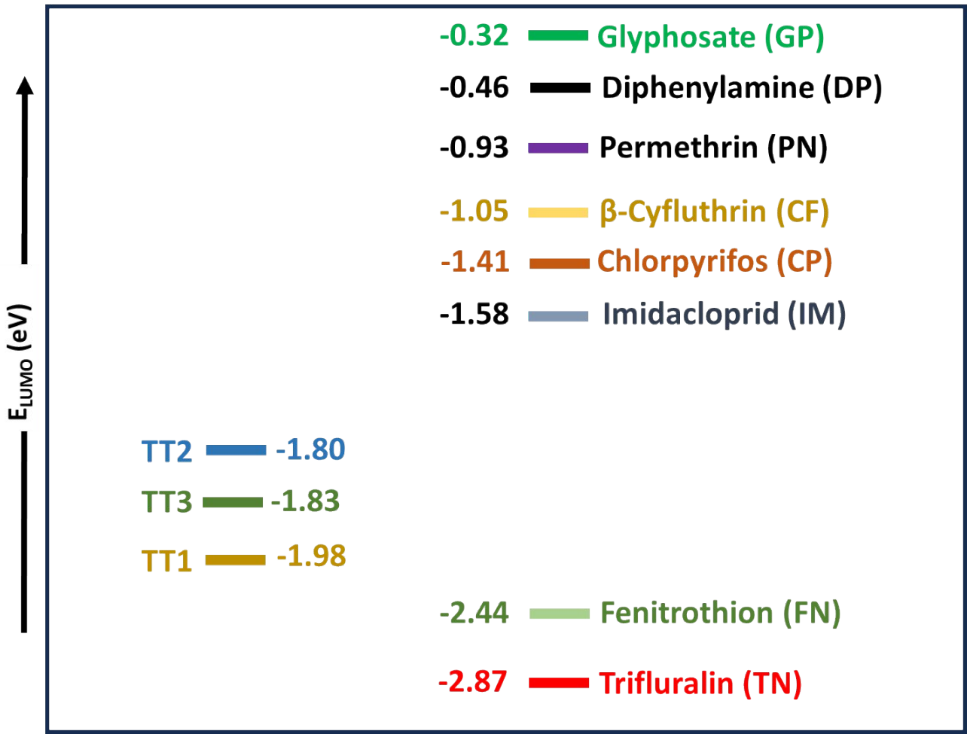

Figure S16. Comparative E_{LUMO} levels of all pesticides and **TT1**, **TT2** and **TT3.** The E_{LUMO} of TN, FN, IM, GP, and CF were known in literature[2] and CP, DP and PN were calculated through DFT.(All the calculations were performed in Gaussian using B3LYP-D3(BJ)/6-31G** (with dispersion corrections).

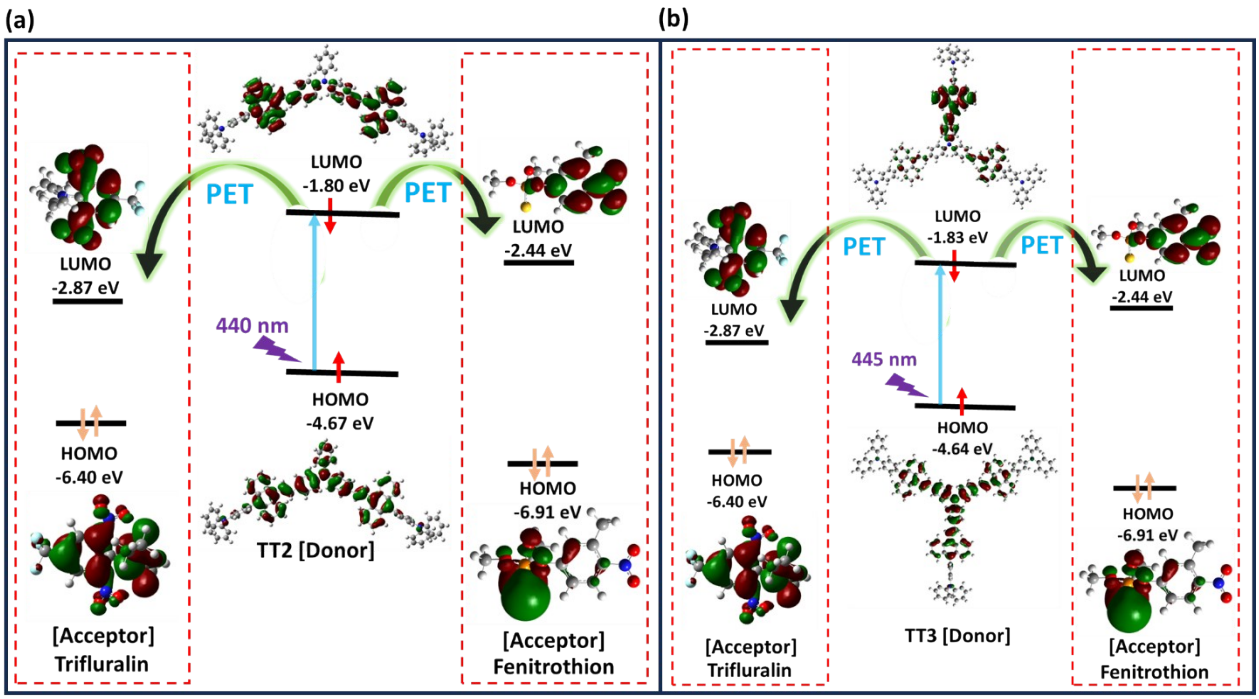

Figure S17. Schematic representation of the photoinduced electron transfer mechanism for (a) **TT2** and (b) **TT3** in the presence of trifluralin and fenitrothion. (All the calculations were performed in Gaussian using B3LYP-D3(BJ)/6-31G** (with dispersion corrections).

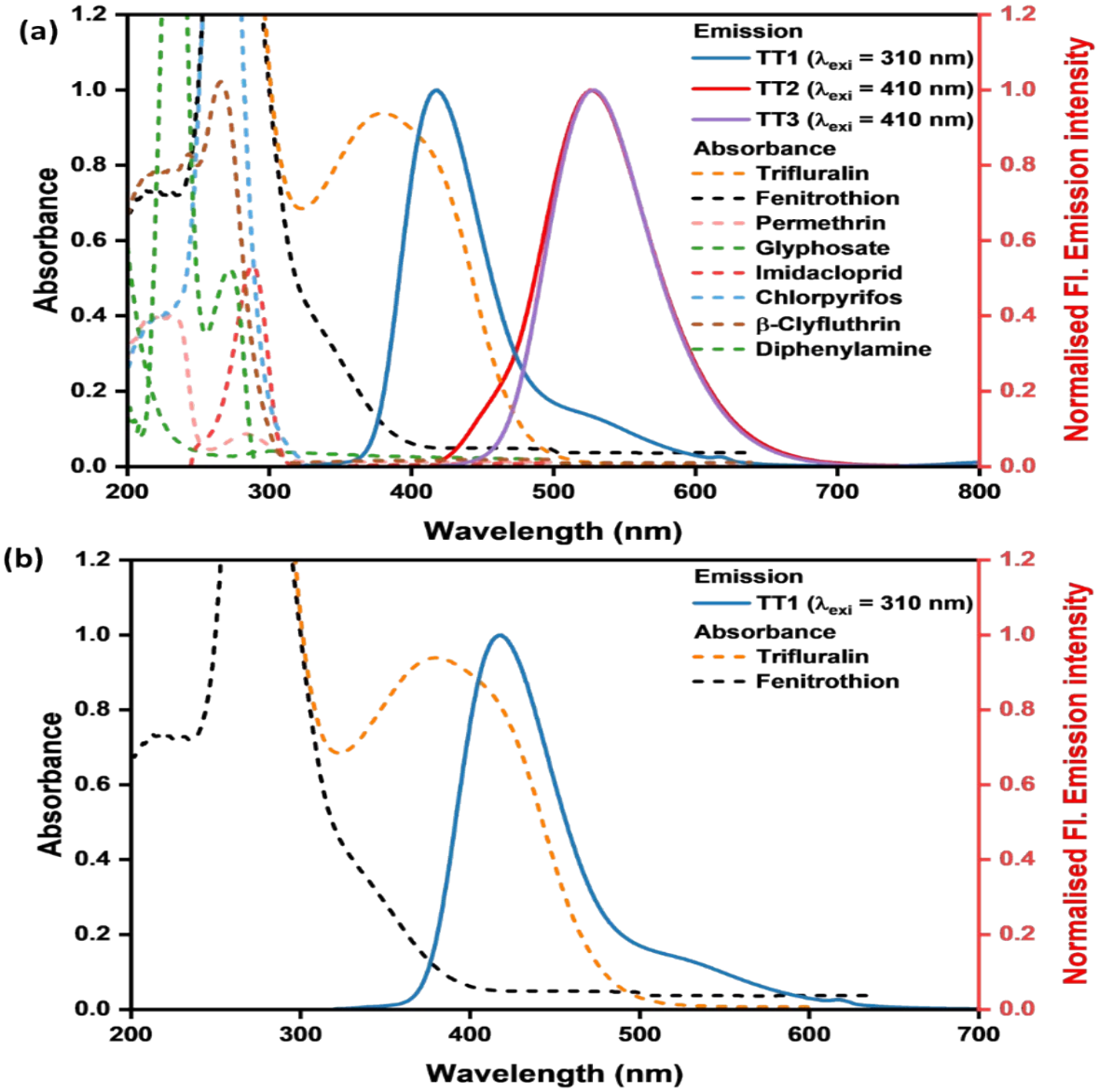

Figure S18. Spectral overlap between absorption and normalised emission bands (a) pesticides and **TT1** (λ_{ex} = 310 nm), **TT2** (λ_{ex} = 410 nm) and **TT3** (λ_{ex} = 410 nm) respectively, (b) TN and FN absorbance overlap with **TT1** emission band.

AIE properties

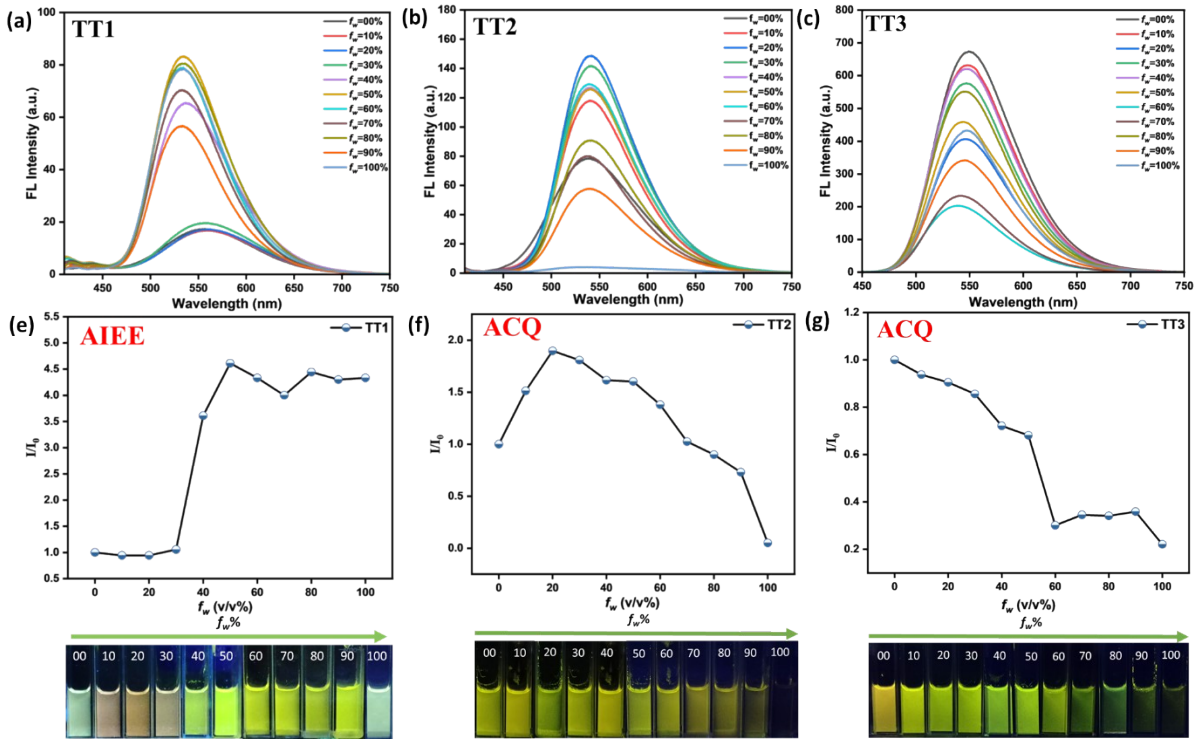

Figure S19. Change in emission of **TT1, TT2** and **TT3** (10 μM) on increasing water fraction.

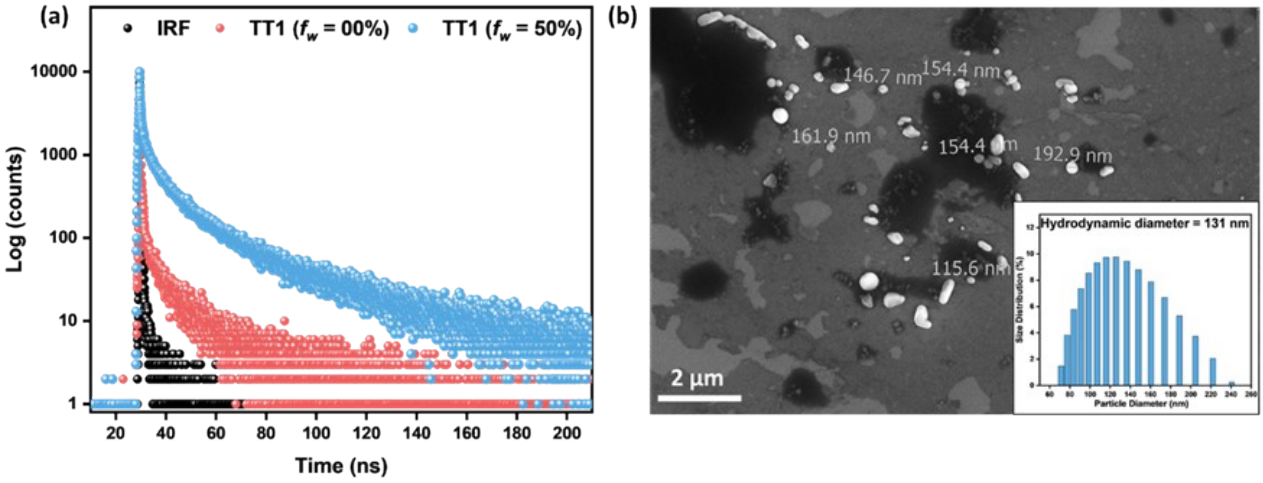

Figure S20. (a) Fl. lifetime decay plot for **TT1 (f_w = 00%) and TT1 (f_w = 50%)**, showing the decay profile for molecular and aggregated states. (b) SEM image for morphology of nanoaggregates and their sizes, and DLS plot for **TT1 (f_w = 50%)** for the hydrodynamic diameter.

Table S5- Fluorescence lifetime decay parameters

Sample	τ_1	τ_2	α_1	α_2	Avg. $<\tau>$	χ^2
TT1 (f_w = 00%)	10.7	1.7	0.15	0.85	**6.41**	1.0
TT1 (f_w = 50%)	2.1	11.2	0.67	0.33	**8.74**	1.1

Absorbance of TT1, TT2 and TT3 in solid state.

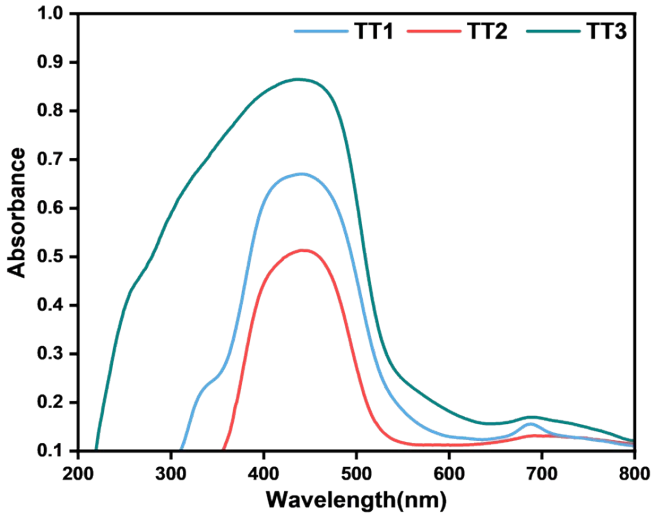

Figure S21. Combined UV-Vis spectrum of **TT1, TT2**, and **TT3** in solid state.

Paper strip characterisation

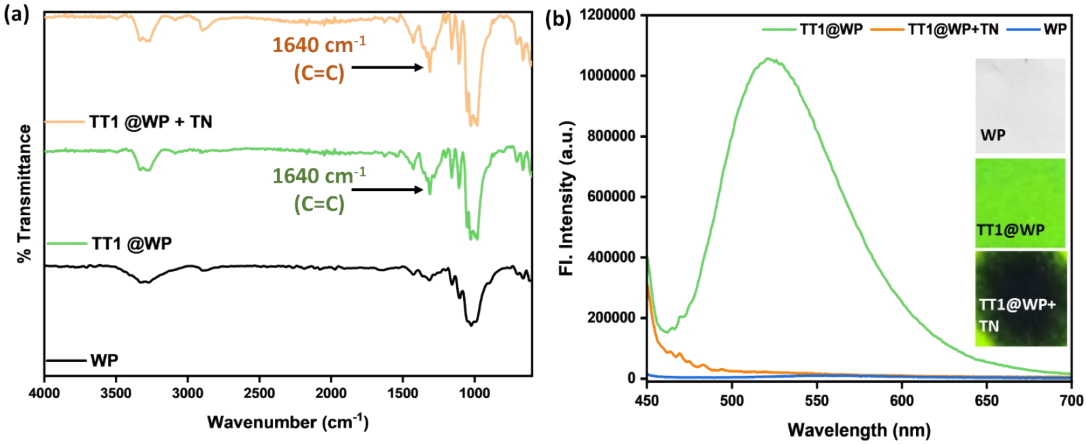

Figure S22. TT1@WP characterisation through (a) IR, and (b) Fluorescence emission spectrum.

Detection of pesticides in the solid state of the probe

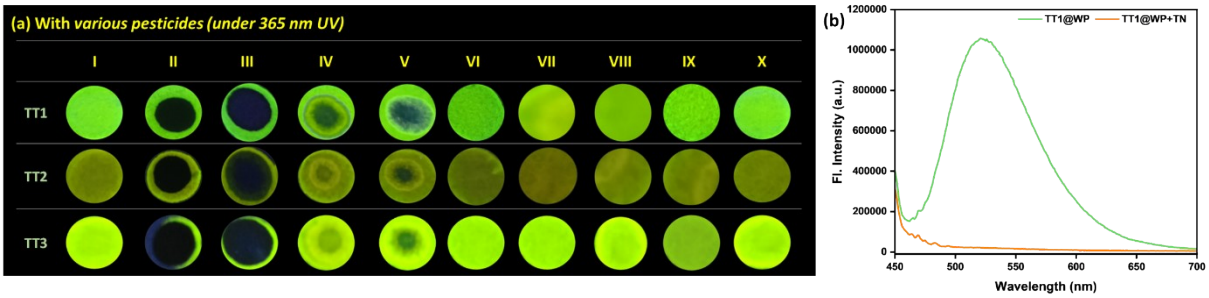

Figure S23. TT1@WP, TT2 @WP and **TT3@WP** (10 μM) before and after exposing various pesticide solutions (under 365 nm UV lamp).Where, I. Probe II. Trifluralin; III: Fenitrothion IV: Glyphosate V. Imidacloprid VI. β-Cyfluthrin; VII. Permethrin VIII. Chlorpyrifos IX: Diphenylamine X: Control (1,4-dioxane)

Schematic diagram for real-life applicability

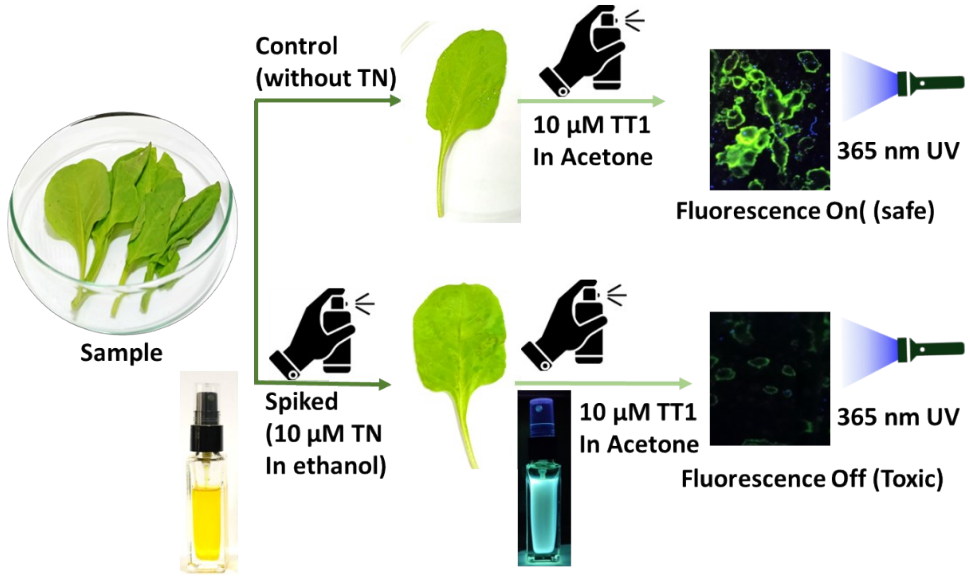

Figure S24. Schematic illustration of experiment for real life applicability of sensor spray.

Fabrication of TT1-coated fluorescent cotton buds

Commercial cotton buds were taken and was cleaned with methanol for removing the chemical residues, further it was dried for 30 min in 40 ^{o}C in hot air oven, the cleaned buds were dipped in **TT1** solution (10 µM in acetone) for 40 minutes, to ensure even absorption of dye in cotton buds, further the cotton buds were separated and was hung freely for 20 minutes with paper

clip to rinse extra **TT1** solution, further the buds were dried at 40 ºC for 30 minutes, and were ready to use.

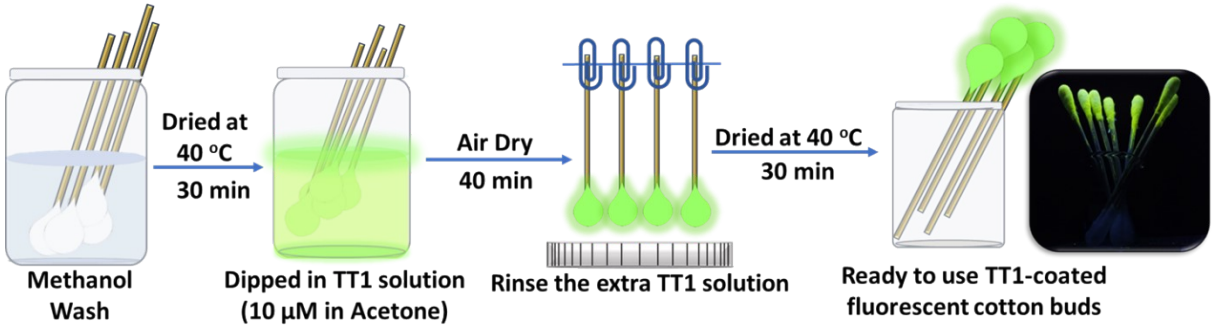

Figure S25. Schematic illustration of the fabrication of **TT1**-coated fluorescent buds.

Table S6: Comparative literature of Trifluralin and Fenitrothion detection

Sl.No.	Reported work	Material	Detection limit (solution)	Detection limit (solid)	Thermal stability (solid)	Response time (solution)	Response time (solid)	Reference
1.	***Efficient Dual-State Visual Detection of Pesticides in Real Samples Using Triphenylamine-Enriched Twisted π-Conjugates***	***Small Molecule***	***180 nM***	***100 nM***	***>300 ºC***	***Rapid***	***Rapid***	***This Work***
2	Creation of Carbazole-Based Fluorescent Porous Polymers for Recognition and Detection of Various Pesticides in Water	Porous organic polymer (POPs)	NA	0.35 µM	NA	Rapid	Rapid	*ACS Sens.* **2020**, *5*, 162–170
3	Synthesis of Fluorescent Micro- and Mesoporous Polyaminals for Detection of Toxic Pesticides	Porous organic polymer (POPs)	NA	6.8 µM	NA	Rapid	Rapid	*Macromolecules* **2018**, *51*, 1769–1776
4	Highly Sensitive and Recognizable Detection for Trifluralin with Alkyl-Decorated Fluorescent Porous Polymers	Porous polymer	6 µM	5 µM	< 250 ºC	4 s	NA	*Chem. Eng. J.* ***2023, 470, 144123.***

5	A Simple AIE Probe to Pesticide Trifluralin Residues in Aqueous Phase: Ultra-Fast Response, High Sensitivity, and Quantitative Detection Utilizing a Portable Platform	Small molecule	6.28 μM	NA	NA	Rapid	NA	*Talanta* ***2024****, 269, 125352.*
6	A practical fluorometric and colorimetric dual-mode sensing platform based on two-dimensional porous organic nanosheets for rapid determination of trifluralin	porous organic nanosheets	3.50 nM	0.41 μM	NA	9 s	NA	*Anal. Methods,* ***2025****,17, 1188-1195*
7	Green Synthesis of Fluorescent Carbon Dots from Cherry Tomatoes for Highly Effective Detection of Trifluralin Herbicide in Soil Samples	carbon quantum dots	0.5 nM	NA	NA	NA	NA	*Chemistry Select* ***2020****, 5 (6), 1956–1960*

Reference

1. Tripathi, S.; Halder, S.; Sivasakthi, P.; Samanta, P. K.; Chakraborty, C.; Chakravarty, M. Sidearms Elongated C3-Symmetric Electrochromic and Electrofluorochromic π-Conjugate: Small Molecule in Efficient Transparent to Black Switching. *Next Mater.* **2025**, *6*, 100472.

2. Zhang, B.; Li, B.; Wang, Z. Creation of Carbazole-Based Fluorescent Porous Polymers for Recognition and Detection of Various Pesticides in Water. *ACS Sens.* **2020**, 5, 162–170.